

1 **The Climate Response to Global Forest Area Changes under Different Warming**
2 **Scenarios in China**

3 Ying HUANG¹, Anning HUANG*^{1,2}, and Jie TAN^{1,3}

4 ¹*School of Atmospheric Sciences, Nanjing University, Nanjing210023, China*

5 ²*Frontiers Science Center for Critical Earth Material Cycling, Nanjing University,*

6 *Nanjing210023, China*

7 ³*Glarun Technology Co., Ltd., Nanjing211106, China*

8 **ABSTRACT**

9 Human activities have notably affected the Earth's climate through greenhouse
10 gases (GHG), aerosol and land use/land cover change (LULCC). To investigate the
11 impact of forest changes on regional climate under different shared socioeconomic
12 pathways (SSPs), we analyzed changes in surface air temperature and precipitation over
13 China under low and medium/high radiative forcing scenarios from 2021 to 2099, using
14 multi-model climate simulations from the Coupled Model Intercomparison Project
15 Phase 6 (CMIP6). Results show that the climate responses to forest changes are more
16 significant under the low radiative forcing scenario. Deforestation would increase the
17 mean, interannual variability, and the trend of surface air temperature under the low
18 radiative forcing scenario, while decreasing those indices under the medium/high
19 radiative forcing scenario. The changes in temperature show significant spatial
20 heterogeneity. For precipitation, under the low radiative forcing scenario, deforestation

*Corresponding author: Anning HUANG
Email: anhuang@nju.edu.cn

21 would lead to a significant increase in northern China and a significant decrease in
22 southern China, respectively, and the effects are persistent in the near-term (2021-2040),
23 middle-term (2041-2070) and long-term (2071-2099). In contrast, under the
24 medium/high radiative forcing scenario, precipitation increases in the near-term and
25 long-term over most parts of China, while decreases in the middle-term, especially in
26 southern, northern and northeast China. The magnitude of precipitation response to
27 deforestation remains comparatively small.

28 **Key words:** Land use/land cover change, deforestation, radiative forcing scenario,
29 regional climate

30 **Article Highlights:**

- 31 ● The temperature and precipitation changes in China due to deforestation have
32 different responses under different climate warming backgrounds, and the
33 responses are more significant under the low radiative forcing scenario.
- 34 ● Deforestation would lead to an increase in the annual mean surface air temperature
35 and its interannual variability and trend in all seasons under the low radiative
36 forcing scenario, and these changes show significant regional differences.
- 37 ● Deforestation would lead to significant increase (decrease) in precipitation in
38 northern (southern) China under the low radiative forcing scenario. In contrast, the
39 responses of temperature and precipitation changes are uncertain under the
40 medium/high radiative forcing scenario.

42 **1. Introduction**

43 IPCC has indicated that greenhouse gases (GHG), aerosol and large-scale land
44 use/land cover change (LULCC) are important anthropogenic activities that induce
45 historical climate change over the past century and are expected to continue to affect
46 future climate (IPCC AR6 chapter 3, 2021). Increasing concentrations of greenhouse
47 gases warm the global atmosphere, intensify the hydrological cycle, and increase
48 precipitation in many regions, whereas LULCC affects the land-atmosphere
49 interactions by altering biophysical processes, which in turn affect regional and global
50 climate (Held and Soden, 2006; Hurtt et al., 2006; Pitman et al., 2009, 2011; Yang et
51 al., 2009; Pielke et al., 2011; Wan et al., 2014; Xu et al., 2015, 2017; Zhu et al., 2018;
52 Huang et al., 2020). While previous modeling and observational studies have shown
53 that the global averaged LULCC impacts on temperature and rainfall are negligible, the
54 regional impacts can be of similar magnitude to CO₂-induced changes, or even stronger
55 and more statistically significant than the CO₂ warming effects (Foley et al., 2005;
56 Arora and Montenegro, 2011; Pitman et al., 2012; Lawrence et al., 2012; Shao and Zeng,
57 2012; Brovkin et al., 2013; Hua et al., 2015; Chen et al., 2015; Yuan and Zhai, 2022).

58 Afforestation is one of the most important human activities causing land use/land
59 cover changes and is an important approach to mitigate global warming. Forests store
60 large amounts of carbon, which is about 1.5 times that stored in the atmosphere (Dixon
61 et al., 1994). The IUFRO report (2009) indicates that the carbon dioxide release from
62 historical deforestation accounts for almost one fifth of the increasing CO₂ in the

63 atmosphere. Previous studies have shown that forests dampen or amplify anthropogenic
64 climate change through the complex and nonlinear forest-atmosphere interactions
65 (Bonan, 2008; Lee et al., 2011; Alkama and Cescatti, 2016). Forests induce important
66 climate forcings and feedbacks. For instance, forests have a lower albedo than other
67 land cover types, which contributes to amplifying local warming through decreasing
68 surface albedo and increasing shortwave radiation (the radiative effect).
69 On the other side, forests promote the hydrologic cycle through evapotranspiration,
70 which causes local cooling (the nonradiative effect) (Pitman et al., 2009; Davin and de
71 Noblet-Ducoudre, 2010; Mao et al., 2011). Li et al. (2015) reported that tropical forests
72 had a strong cooling effect throughout the year, temperate forests showed moderate
73 cooling (warming) in summer (winter) with net cooling effect annually, and boreal
74 forests had strong warming in winter and a moderate cooling in summer with net
75 warming effect annually. Such forests-induced spatiotemporal differences in
76 temperature responses result from the divergent changes of the radiative effect (albedo)
77 and the nonradiative effect (evapotranspiration) in different regions. In general, the
78 radiative effect of forests tends to dominate at high latitudes while the nonradiative
79 effect is more important over the tropics. The radiative and nonradiative effects tend to
80 counterbalance each other in the temperate forests (Perugini et al., 2017).

81 Evidence from both observations (Yang et al., 2010; Duveiller et al., 2018; Ge et
82 al., 2019) and climate models (Davin and de Noblet-Ducoudre, 2010; Lorenz et al.,
83 2016; Boysen et al., 2020) has shown that the biophysical impact of deforestation
84 warms the tropics and cool the boreal regions, while the response of deforestation in

85 the mid latitude is uncertain. Li et al. (2016) suggested that the latitudinal pattern of
86 temperature response depends nonlinearly on the spatial extent and the intensity of
87 deforestation. Temperature change in global deforestation is greatly amplified in
88 temperate and boreal regions but is dampened in tropical regions. These divergent
89 temperature patterns reveal the importance of the background climate in modifying the
90 deforestation impact. For precipitation, deforestation can impact precipitation through
91 biophysical processes, which leads to decreased annual average precipitation, reduced
92 heavy precipitation frequency/intensity, and shortened duration of rainy seasons over
93 the deforested areas (Luo et al., 2022).

94 To address the growing environmental concerns and deal with global warming,
95 China has developed the Three-North Shelterbelt Development Program, the Natural
96 Forest Conservation Program, and the Grain for Green Program, and plans to expand
97 afforestation in the near future (Liu et al., 2008; Fu et al., 2017; Bryan et al., 2018).
98 Therefore, investigation of the overall climate impact of global forest changes over
99 China is one strategy demand for China's afforestation policies. Due to the uncertain
100 effects of forest changes on regional temperature and precipitation through biophysical
101 and biochemical processes, the regional impacts of LULCC depend not only on the
102 background climate but also on the background climate change (Pielke and Avissar,
103 1990; Taylor et al., 2002; Sun and Mu, 2013; Hua et al., 2017). Pitman et al. (2011)
104 noted that the increasing greenhouse gases caused changes in snow and rainfall, which
105 affect the snow-albedo feedback and the water supply, which in turn limits evaporation.
106 The above changes largely control the net impact of LULCC on regional climate. The

107 LULCC-induced radiative forcing (RF) is different under different background
108 climates with GHG concentrations in 1850 and in the present age, thus leading to
109 different temperature and precipitation responses to LULCC (Hua and Chen, 2013;
110 Hu et al., 2018). Will the regional impact of afforestation be different in China during
111 global warming, and which part has the strongest effects? These effects require further
112 investigation, but remain poorly understood analysis at present.

113 Along with human social activities and economic development, will future
114 increasing greenhouse gases emissions and expanding LULCC result in increased
115 precipitation and temperature, and more significant regional climate effects? These
116 require further exploration. Therefore, CMIP6 has endorsed the Land Use Model
117 Intercomparison Project (LUMIP). The LUMIP model experiments have been
118 developed in consultation with several existing model intercomparison activities and
119 research programs that focus on the biogeophysical impact of land use on climate. The
120 simulations can be used to quantify the historic impact of land use and explore the
121 potential for future land management decisions to aid in mitigation of climate change
122 (Lawrence et al., 2016). The impact of the different land use scenarios on the future
123 climate, especially on the regional climate, has implications for understanding the role
124 of land use and land management in regional climate mitigation (Hong et al., 2022). In
125 this study, we aim to investigate the impact of changes in forest area under different
126 emissions scenarios on regional climate over China by using LUMIP multi-model
127 climate simulations. The analyses of the future global deforestation experiments could
128 advance our understanding of deforestation-induced climate changes, and provide new

129 guidance to afforestation strategies and climate change mitigation policy.

130 2. Data and method

131 2.1 Data

132 In this study, we used monthly precipitation and surface air temperature (SAT)
133 data from 5 climate models that participate in the Coupled Model Intercomparison
134 Project Phase 6 (CMIP6) (Table 1), including historical runs, Scenario Model
135 Intercomparison Project (ScenarioMIP) and Land-Use Model Intercomparison Project
136 (LUMIP). For ScenarioMIP, we selected two future scenarios: SSP1-2.6 and SSP3-7.0
137 (global radiative forcing of 2.6 and 7.0 $\text{W} \cdot \text{m}^{-2}$ by 2100, respectively) from 2015 to 2100.
138 For LUMIP, the two future land-use policy sensitivity experiments (i.e., SSP370-
139 SSP126Lu and SSP126-SSP370Lu) from 2015 to 2099 were used (Table 2).

140 **Table 1.** Basic information for the used CMIP6 models.

Model name	Institution/Country	Resolution (Lon × Lat)
ACCESS-ESM1-5	CSIRO/Australia	1.875° × 1.25°
BCC-CSM2-MR	BCC/China	T106 (1.125° × 1.125°)
CMCC-ESM2	CMCC/Italy	1.25° × 0.938°
MPI-ESM1-2-LR	MPI-M/Germany	T63 (1.875° × 1.875°)
NorESM2-LM	NCC/Norway	2.5° × 1.875°

141 **Table 2.** CMIP6 datasets

Experiment ID	Experiment name	Experiment description	Years
Historical	Historical	Concentration driven (consistent with observations from 1850-2005)	1961~2014
SSP1-2.6	ScenarioMIP	Low radiative forcing scenario, Radiative forcing reaches a level of 2.6W/m ² in 2100	2015~2100
SSP3-7.0	ScenarioMIP	Medium/high radiative forcing scenario,	2015~2100

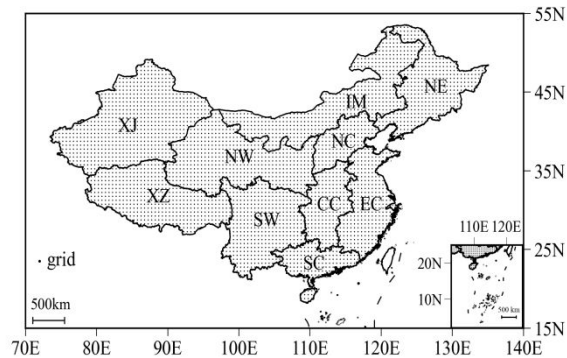
		Radiative forcing reaches a level of 7.0 W/m ² in 2100	
SSP126-SSP370Lu	LUMIP	Same as ScenarioMIP <i>ssp126</i> except use land use from <i>ssp370</i> (SSP3-7 deforestation scenario)	2015~2099
SSP370-SSP126Lu	LUMIP	Same as ScenarioMIP <i>ssp370</i> except use land use from <i>ssp126</i> (SSP1-2.6 afforestation scenario)	2015~2099

142 LUMIP experiments are derivatives of ScenarioMIP (SSP3-7.0 and SSP1-2.6)
143 simulations. This particular set of simulations was selected because the projected land-
144 use trends in SSP3-7.0 and SSP1-2.6 diverge strongly, with SSP3-7.0 representing a
145 reasonably strong deforestation scenario (global forest area decreases from 38 million
146 km² to 33 million km² during 2015-2100), while SSP1-2.6 including significant
147 afforestation (global forest area increases from 37 million km² to 43 million km² during
148 2015-2100). Within the LUMIP framework, these simulations design concentration-
149 driven variants of ScenarioMIP SSP3-7.0 and SSP1-2.6, but each uses the land-use
150 scenario from the other. SSP370-SSP126Lu experiment runs with all forcings identical
151 to SSP3-7.0, except that the land use is taken from SSP1-2.6. In contrast, SSP126-
152 SSP370Lu experiments use all forcing from SSP1-2.6, except for the land use from
153 SSP3-7.0. The LUMIP experiments are described in detail in Lawrence et al. (2016).

154 **2.2 Division of subregions**

155 To examine the regional differences in impacts, China is divided into ten
156 subregions: NE (northeast China), NC (north China), IM (Inner Mongolia), CC (central
157 China), EC (east China), SC (south China), SW (southwest China), NW (northwest
158 China), XZ (Xizang), and XJ (Xinjiang) according to administrative boundaries as well

159 as on geographical and societal conditions (Fig. 1).



160

161 **Fig. 1.** The division of the ten subregions (NE: northeast China; NC: north China; IM:
162 Inner Mongolia; EC: east China; CC: central China; SC: south China; SW: southwest
163 China; NW: northwest China; XZ: Xizang; and XJ: Xinjiang).

164 **2.3 Quantification of the regional impact of deforestation**

165 We used SSP126-SSP370Lu minus SSP1-2.6, and SSP3-7.0 minus SSP370-
166 SSP126Lu to represent the response of deforestation under the low and medium/high
167 radiative forcing scenarios, respectively. We compared the LULCC effects
168 in two scenarios to examine the extent to which the impact of deforestation differs at
169 different levels of climate change (Lawrence et al., 2016; Hua et al., 2021; Wang et al.,
170 2021).

171 Given the different horizontal resolutions across the models, all model outputs
172 were bilinearly interpolated to the horizontal resolution of $0.5^{\circ} \times 0.5^{\circ}$, and the ensemble
173 mean was used in the analyses. To determine the statistical significance of
174 deforestation-induced changes, we applied the Student's *t*-test to each grid cell.

175 Regional differences of deforestation-induced changes are represented by root
176 mean square error (RMSE), spatial correlation coefficient (SCC), and spatial standard

177 deviation ratios (SSD). In addition, we used the composite evaluation index
178 (Schuenemann and Cassano 2009; Tian et al., 2016) that combines the three indicators,
179 RMSE, SCC, and SSD as follow:

$$180 \quad M_R = 1 - \frac{\sum_{i=1}^n r_i}{1 \times n \times m} \quad (1)$$

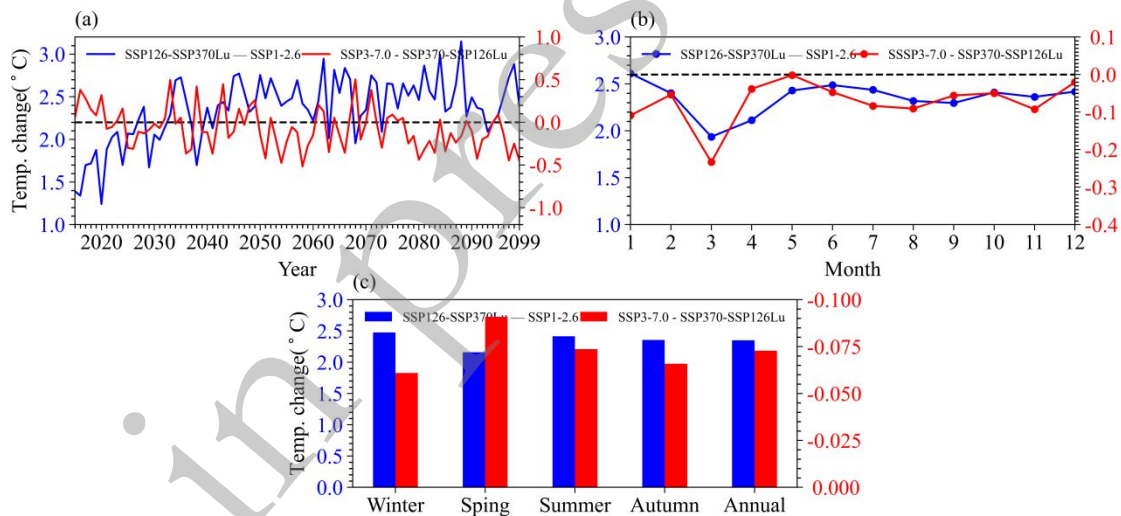
181 Where m is the number of subregions, and n is the number of indicators, r_i denotes the
182 rank of each subregion for a certain indicator and ranges between 1 and m . If the r_i is
183 equal to 1, representing deforestation has minimal impact on local temperature change
184 in a certain subregion, while a larger value of r_i corresponds to a larger response to
185 deforestation. With this method, M_R can represent the overall impact of deforestation
186 on local temperature change, with a smaller value in a certain subregion representing a
187 greater impact of deforestation on temperature change.

188 **3. Results**

189 **3.1 Changes in surface air temperature (SAT)**

190 The deforestation-induced SAT change in China under different radiative forcing
191 scenarios is of specific concern. Under the low radiative forcing scenario, the annual
192 mean SAT changes due to deforestation show a continuing upward trend, with the
193 magnitude of 1.0~3.5°C (Fig. 2). In contrast, the magnitude of deforestation-induced
194 changes is comparatively small under the medium/high radiative forcing scenario,
195 which indicates that the mean SAT response due to deforestation is more significant
196 under the low radiative forcing scenario (Fig. 2a). At the monthly time scales, we find
197 a net warming effect of deforestation by 1.5~3.0°C under the low radiative forcing

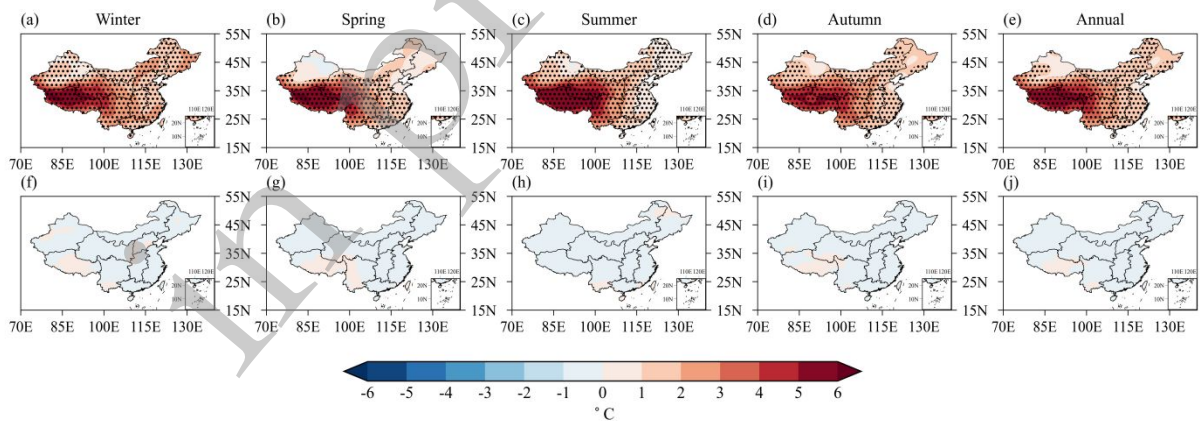
198 scenario, which is largest in January and smallest in March. However, the SAT is
 199 slightly cooling ($-0.2\sim 0^{\circ}\text{C}$) under the medium/high radiative forcing scenario, and the
 200 cooling is strongest in March and weakest in May. Our results indicate that the response
 201 of monthly SAT to the same deforestation can be opposite under different radiative
 202 forcing scenarios (Fig. 2b). At the seasonal time scales, model ensemble mean shows
 203 significant warming ($>2^{\circ}\text{C}$) induced by deforestation under the low radiative forcing
 204 scenario, while it shows a slight cooling ($<-0.1^{\circ}\text{C}$) under the medium/high radiative
 205 forcing scenario (Fig. 2c). Overall, at the annual, monthly, and seasonal time scales, the
 206 SAT response to LULCC is much smaller under the medium/high radiative forcing
 207 scenario than the low radiative forcing scenario.



208
 209 **Fig. 2.** Deforestation-induced regional averaged surface air temperature (SAT) changes
 210 ($^{\circ}\text{C}$) over China under different emissions scenarios. (a) time series from 2015 to 2099,
 211 (b) monthly mean during 2015-2099, and (c) seasonal (DJF, MAM, JJA, and SON)
 212 mean during 2015-2099. Blue: the low radiative forcing scenario, with values in the left
 213 y axis; Red: the medium/high radiative forcing scenario, with values in the right y axis.

214 Analyses from CMIP6 ScenarioMIP simulations show that compared with the

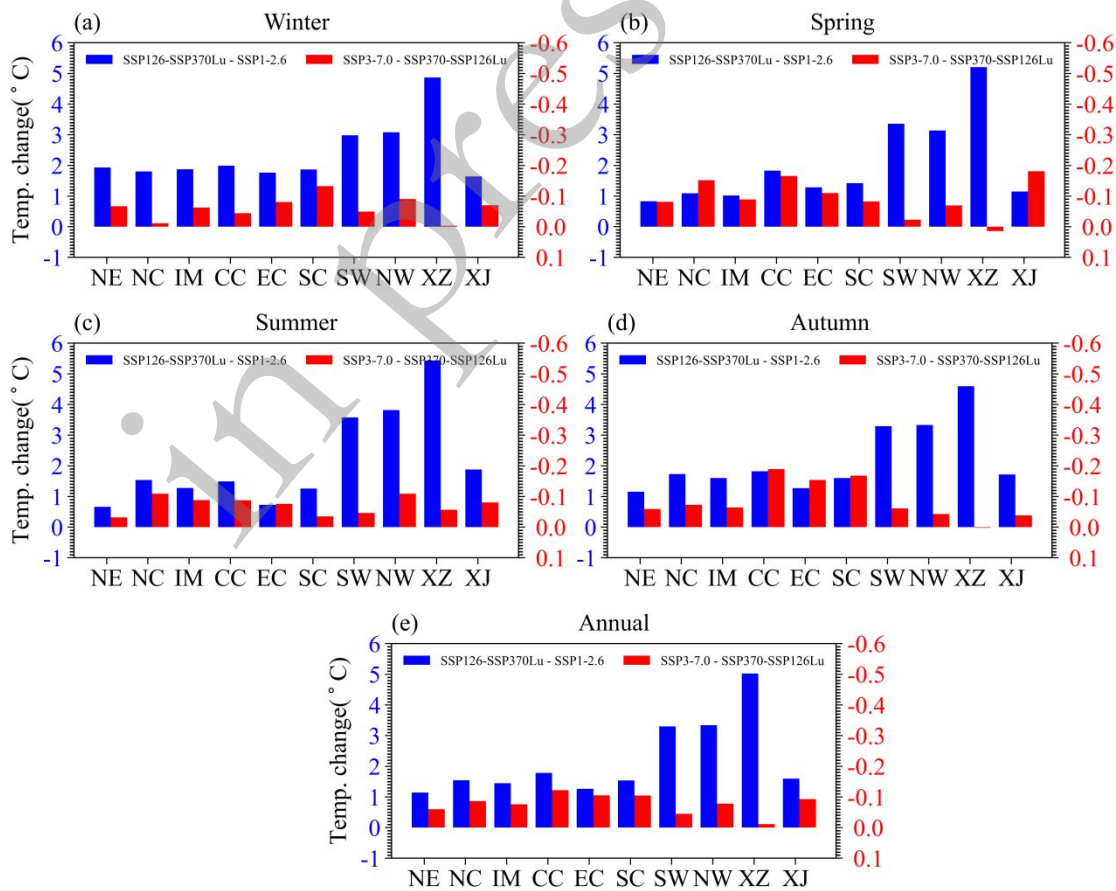
215 historical period, greenhouse gases emissions warm most parts of China throughout a
 216 year. The SAT increase in northern China is larger than that in southern China, and a
 217 higher radiative forcing scenario would cause more warming (Figure not shown).
 218 Further analysis regarding the deforestation effects shows more differences between
 219 the low and medium/high radiative forcing scenarios (Fig. 3). Under the low radiative
 220 forcing scenario, deforestation-induced SAT anomaly show statistically significant
 221 warming in all seasons, especially over the Tibetan Plateau. However, under the
 222 medium/high radiative forcing scenario, deforestation has small impact on SAT in
 223 China and causes cooling in most regions. Thus, under the low radiative forcing
 224 scenario, the impact of deforestation would further amplify the effects of greenhouse
 225 gases in China, while the response of SAT is weak under the medium/high radiative
 226 forcing scenario.



227
 228 **Fig. 3.** Deforestation-induced annual and seasonal (DJF, MAM, JJA, and SON) mean
 229 SAT changes (°C) during 2015-2099 over China under (a-e) the low radiative forcing
 230 scenario, and (f-j) the medium/high radiative forcing scenario. The black dots indicate
 231 changes are statistically significant at a 0.05 confidence level.

232 Figure. 4 presents the mean SAT changes of ten subregions in all seasons to further

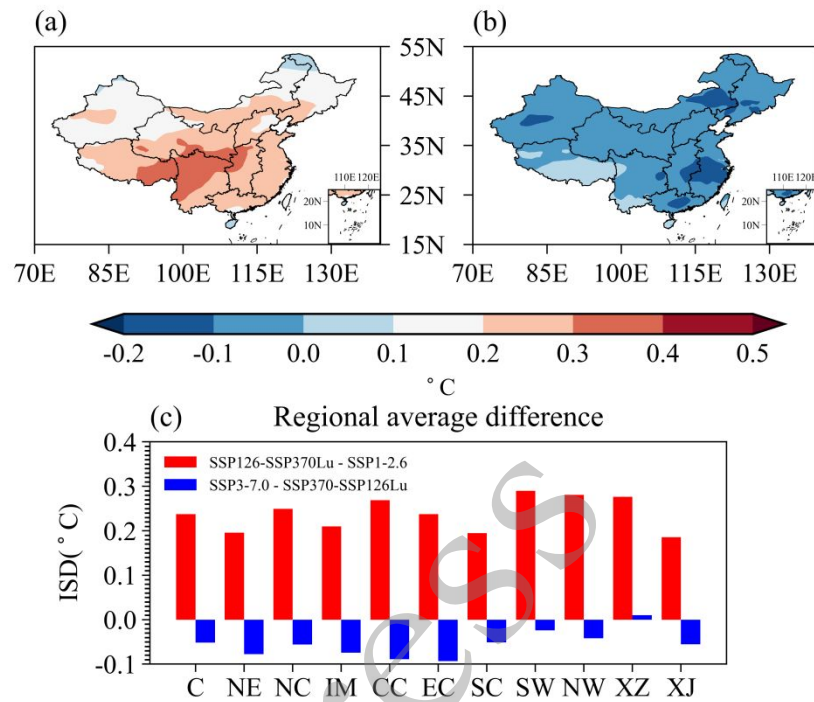
233 examine the regionally different effects of deforestation. Under the low radiative
 234 forcing scenario, the deforestation-induced SAT changes are positive in all subregions
 235 and have obvious regional differences. In particular, the positive SAT changes in
 236 southwest China (SW), northwest China (NW) and Xizang (XZ) are significantly
 237 greater than those in other subregions in all seasons, which indicate deforestation would
 238 lead to more significant warming in these subregions under the low radiative forcing
 239 scenario. In contrast, under the medium/high radiative forcing scenario, except for
 240 Xizang (XZ) in spring, other subregions have negative SAT changes in all seasons, that
 241 is, deforestation would cause cooling effects under the medium/high radiative forcing
 242 scenario, but the magnitude of cooling is slight (no more than -0.3C).



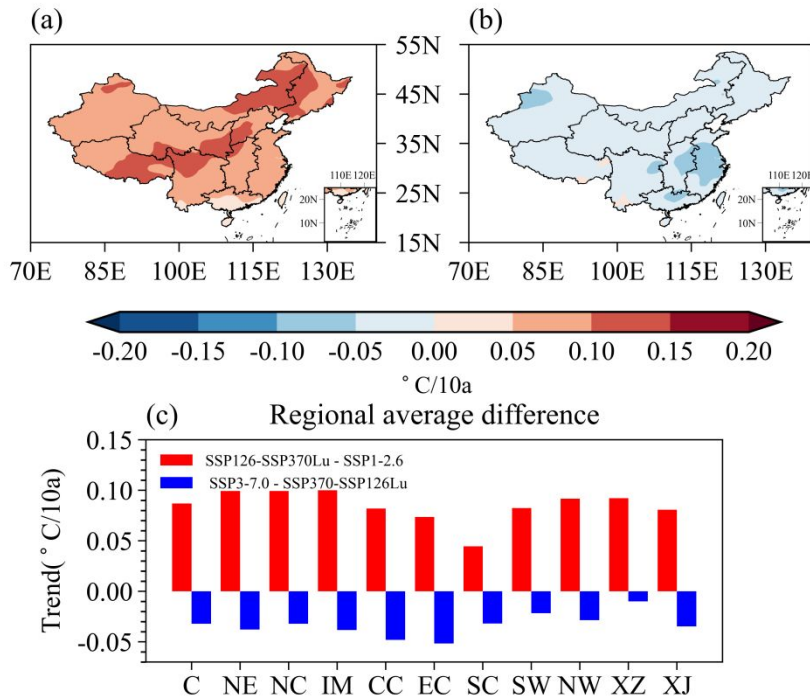
243

244 **Fig. 4.** Deforestation-induced subregional annual and seasonal (DJF, MAM, JJA, and

245 SON) mean SAT changes ($^{\circ}\text{C}$) during 2015-2099 under different emissions scenarios
 246 (blue bar: the low radiative forcing scenario, with values in the left y axis; red bar: the
 247 medium/high radiative forcing scenario, with values in the right y axis).



248
 249 **Fig. 5.** Deforestation-induced interannual variability of SAT change ($^{\circ}\text{C}$) during 2015-
 250 2099 under (a) the low radiative forcing scenario, (b) the medium/high radiative forcing
 251 scenario, and (c) average over China (C) and the ten subregions.



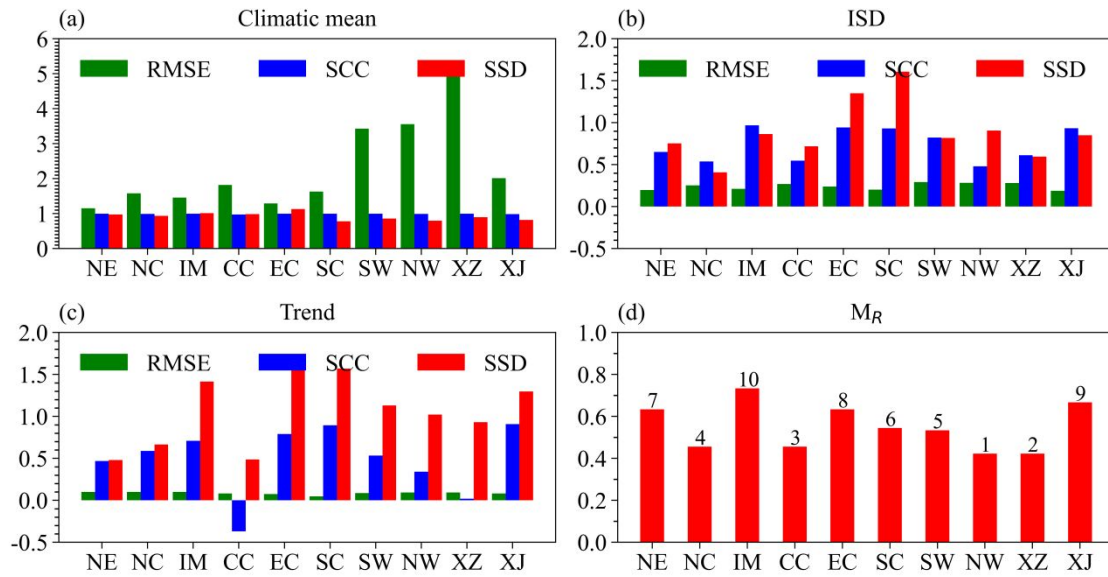
252

253 **Fig. 6.** As in Fig. 5, but for the trend of surface air temperature change (°C/10a).

254 Except for the mean SAT changes, we also analyze deforestation effects on
 255 interannual variability (Fig. 5) and trend (Fig. 6) of SAT under different warming
 256 scenarios. Under the low radiative forcing scenario, deforestation leads to an increase
 257 in the interannual variability of SAT, especially in southwest China and the eastern part
 258 of the Tibetan Plateau (Fig. 5a). The trend of SAT in China also shows significant
 259 increase, especially in eastern China, which exceeds 0.1°C/10a (Fig. 6a). In contrast,
 260 under the medium/high radiative forcing scenario, the opposite response due to
 261 deforestation would decrease the interannual variability (Fig. 5b) and the trend of SAT
 262 (Fig. 6b) in most subregions. For each subregion, deforestation leads to an increase in
 263 interannual variability and trend of SAT of similar magnitude under the low radiative
 264 forcing scenario. While under the medium/high radiative forcing scenario, the response
 265 is opposite except for in Xizang subregion. The interannual variability of mean SAT

266 decreases in all subregions, and the magnitude is smaller than that under the low
267 radiative forcing scenario (Fig. 5c). The analysis of SAT trend in subregions also
268 reaches similar conclusions (Fig. 6c).

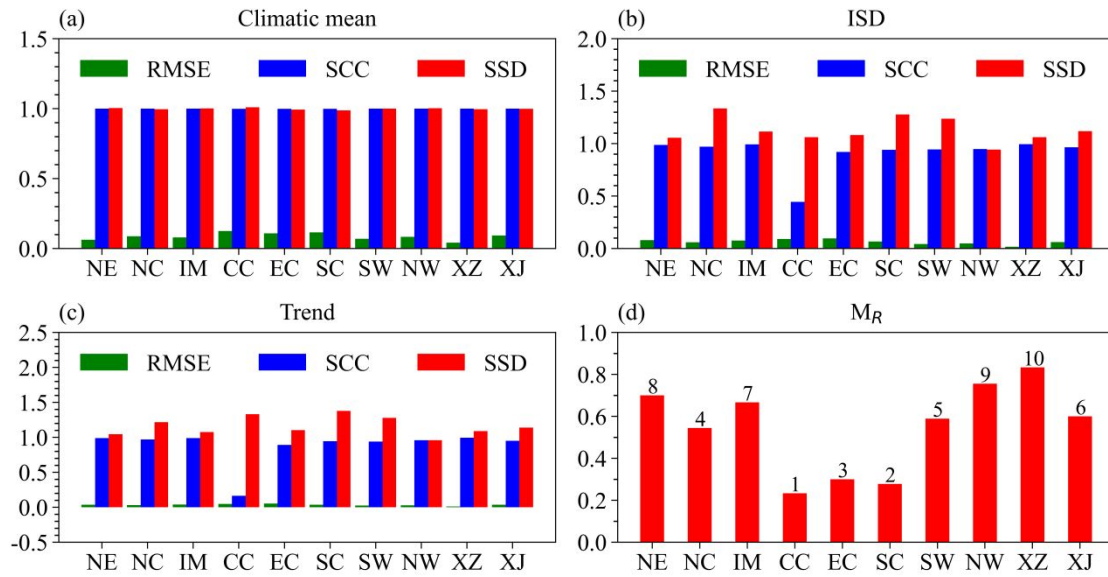
269 To quantitatively compare the response of SAT to deforestation in different
270 subregions under different scenarios, we calculate the indices (RMSE, SCC, and SSD)
271 of mean SAT and its interannual variability and trend. When RMSE is smaller (larger),
272 SCC is larger (smaller), and SSD is closer to (far away from) 1, which means the SAT
273 of a certain subregion is less (more) affected by deforestation. Under the low radiative
274 forcing scenario, the RMSE of mean SAT has obvious regional differences, especially
275 in Xizang, northwest and southwest China. The SCC of each subregion is more than
276 0.9 with similar magnitude among different subregions. The value of SSD ranges from
277 0.78 to 1.13, which means that the spatial consistency and similarity of mean SAT are
278 high (Fig. 7a). The interannual variability and trend of SAT are also analyzed in a
279 similar way. We find the RMSE of the interannual variability is similar in different
280 regions, while the SCC and SSD are significantly different regionally. The SCC in Inner
281 Mongolia, east China, south China and Xinjiang exceeds 0.9, while the SCC in
282 northwest China is about 0.4. The SSDs in Inner Mongolia, northwest China, and
283 Xinjiang are close to 1, while the values in south and east China are far away from 1
284 (Fig. 7b).



285

286 **Fig. 7.** Regional averaged changes of deforestation-induced during 2015-2099 under
 287 the low radiative forcing scenario. (a) mean SAT ($^{\circ}\text{C}$), (b) interannual variability ($^{\circ}\text{C}$),
 288 and (c) trend ($^{\circ}\text{C}/10\text{a}$); and (d) M_R value of ten subregions. Green, blue and red bar in
 289 (a-c) denote RMSE, SCC and SSD, respectively. The number above the bar in (d)
 290 denote the response to deforestation with descending sequence over ten subregions
 291 under the low radiative forcing scenario.

292 The RMSE of the trend of SAT in each subregion is small, and the regional
 293 differences are not significant. However, the SCC and SSD both have obvious regional
 294 differences, with the largest positive value of SCC in Xinjiang and south China and the
 295 negative value in central China. SSD is close to 1 in Xizang, southwest, and northwest
 296 China, while the value is the far away from 1 in Inner Mongolia, east and south China
 297 (Fig. 7c). In terms of the composite evaluation index M_R , a smaller value represents a
 298 greater impact of deforestation on the regional SAT. Under the low radiative forcing
 299 scenario, we find the most significant SAT response to deforestation in northwest China,
 300 and the smallest impact in Inner Mongolia (Fig. 7d).



301

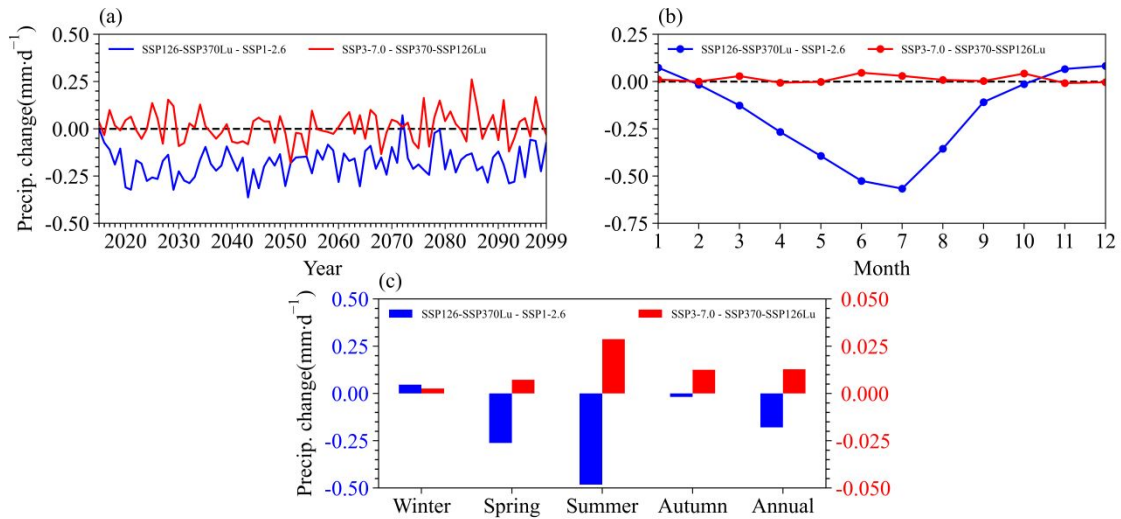
302 **Fig. 8.** As in Fig. 7, but under the medium/high radiative forcing scenario.

303 Figure. 8 shows the same analysis under the medium/high radiative forcing
 304 scenario. For the mean SAT, the RMSE of each subregion is small and the SCC and
 305 SSD are both close to 1, indicating no obvious regional differences. Therefore,
 306 deforestation has little impact on mean SAT changes in China under the medium/high
 307 radiative forcing scenario, which is quite different from that under the low radiative
 308 forcing scenario (Fig. 8a). The analyses of the interannual variability (Fig. 8b) and the
 309 trend of SAT (Fig. 8c) also obtain similar conclusions. Under the medium/high
 310 radiative forcing scenario, the RMSE is small and there are no obvious regional
 311 differences. The SCC and SSD in all subregions are close to 1 except in central China,
 312 indicating that deforestation has little impact on the interannual variability and trends
 313 of SAT. The value of M_R for each subregion are sequenced in ascending order: central
 314 China, south China, east China, north China, southwest China, Xinjiang, Inner
 315 Mongolia, northeast China, northwest China and Xizang. Thus, under the medium/high
 316 radiative forcing scenario, deforestation has the largest impact on SAT in central China,

317 and the smallest impact in Xizang subregion (Fig. 8d).

318 ***3.2 Changes in precipitation***

319 We also examine the impacts of deforestation on precipitation under different
320 radiative forcing scenarios (Fig. 9). Under the low radiative forcing scenario,
321 deforestation leads to a significant decrease in annual precipitation, while the
322 precipitation has no obvious trend under the medium/high radiative forcing scenario
323 (Fig. 9a). Our results indicate the impact of deforestation on annual precipitation is
324 uncertain under the medium/high radiative forcing scenario. At the monthly scale, the
325 precipitation changes under different scenarios are basically opposite (Fig. 9b). Under
326 the low radiative forcing scenario, deforestation leads to decreased precipitation in most
327 months except for January, November, and December. The largest reduction is found
328 in July, reaching approximate $-0.5 \text{ mm} \cdot \text{d}^{-1}$. However, under the medium/high radiative
329 forcing scenario, we find slightly increase in deforestation-induced precipitation. At the
330 seasonal scale, deforestation-induced precipitation changes are opposite under different
331 forcing scenarios except for in winter. The most significant changes are found in
332 summer in both scenarios, and the impact of deforestation on precipitation is more
333 significant than under the low radiative forcing scenario (Fig. 9c).



334

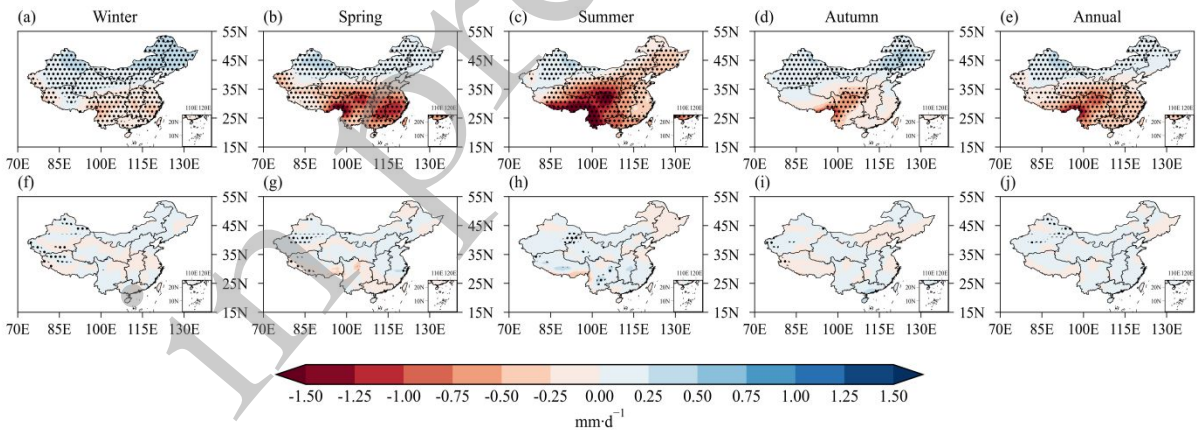
335 **Fig. 9.** Deforestation-induced regional averaged precipitation change ($\text{mm}\cdot\text{d}^{-1}$) over

336 China under different emissions scenarios. (a) time series from 2015 to 2099, (b)

337 monthly mean during 2015-2099, and (c) seasonal (DJF, MAM, JJA, and SON) mean

338 during 2015-2099. Blue: the low radiative forcing scenario, with values in the left y

339 axis; Red: the medium/high radiative forcing scenario, with values in the right y axis.



340

341 **Fig. 10.** Deforestation-induced annual and seasonal (DJF, MAM, JJA, and SON) mean

342 precipitation changes ($\text{mm}\cdot\text{d}^{-1}$) during 2015-2099 over China under (a-e) the low

343 radiative forcing scenario, and (f-j) the medium/high radiative forcing scenario. The

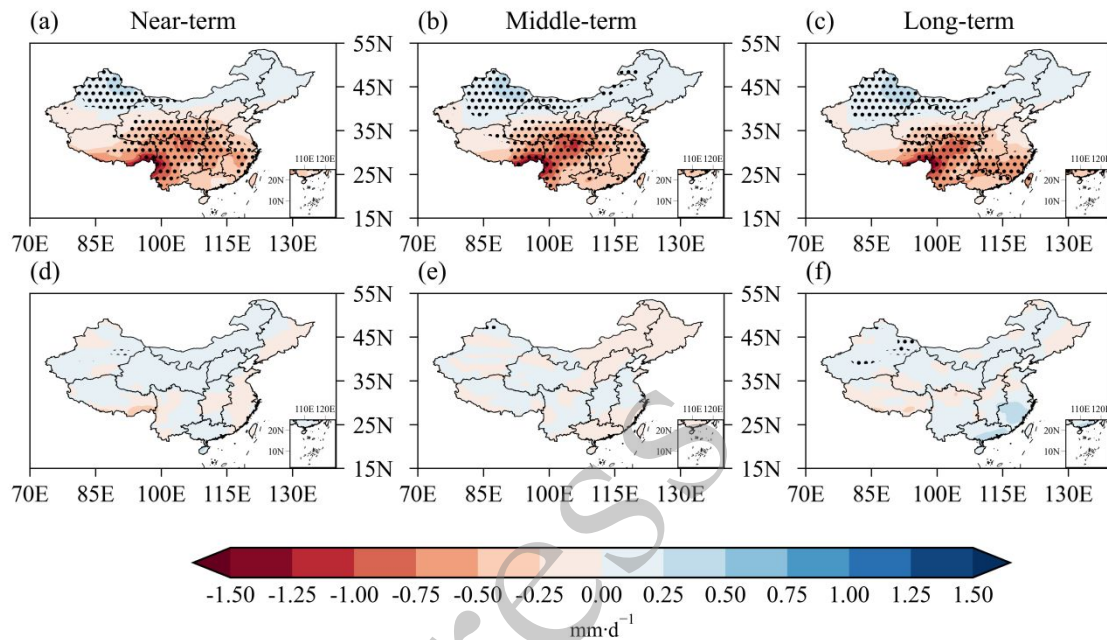
344 black dots indicate changes are statistically significant at a 0.05 confidence level.

345 We further analyze the impact of deforestation on the regional differences of

346 seasonal precipitation in China under different warming scenarios. Under the low
347 radiative forcing scenario, deforestation would lead to a significant decrease (increase)
348 in precipitation in southern (northern) China in winter (Fig. 10a), spring (Fig. 10b), and
349 autumn (Fig. 10d). In summer (Fig. 10c), the precipitation decreases in most parts of
350 China except for Xinjiang, especially in southwest China and Xizang ($>1.5 \text{ mm}\cdot\text{d}^{-1}$).
351 However, under the medium/high radiative forcing scenario, the regional impact of
352 deforestation on seasonal precipitation in China is uncertain, and the precipitation
353 changes in most regions are not significant (Fig. 10f-j).

354 The spatial patterns of precipitation anomaly are divided into three periods: near-
355 term (2021-2040), middle-term (2041-2070), and long-term (2071-2099). In the three
356 periods, the difference of forest area between the low and medium/high radiative
357 forcing scenario is about $2\times 10^6 \text{ km}^2$, $5\times 10^6 \text{ km}^2$, and $8\times 10^6 \text{ km}^2$, respectively. Figure.11
358 shows the spatial patterns of deforestation-induced precipitation anomaly in China
359 under different warming backgrounds. Under the low radiative forcing scenario, the
360 spatial pattern of deforestation-induced precipitation anomaly is similar in the three
361 periods, with a significant decrease in southern China and increase in northern China,
362 especially in Xinjiang. As we know, under the ScenarioMIP SSP1-2.6 scenario, global
363 warming would lead to decreased precipitation in winter in southern China while
364 increased precipitation in other seasons over most parts of China. In the near-term, there
365 is precipitation decreases in southern China and increases in northern China, while in
366 the middle-term and the long-term, precipitation increases in most subregions (Figure
367 not shown). Compared with the ScenarioMIP SSP1-2.6 scenario, deforestation would

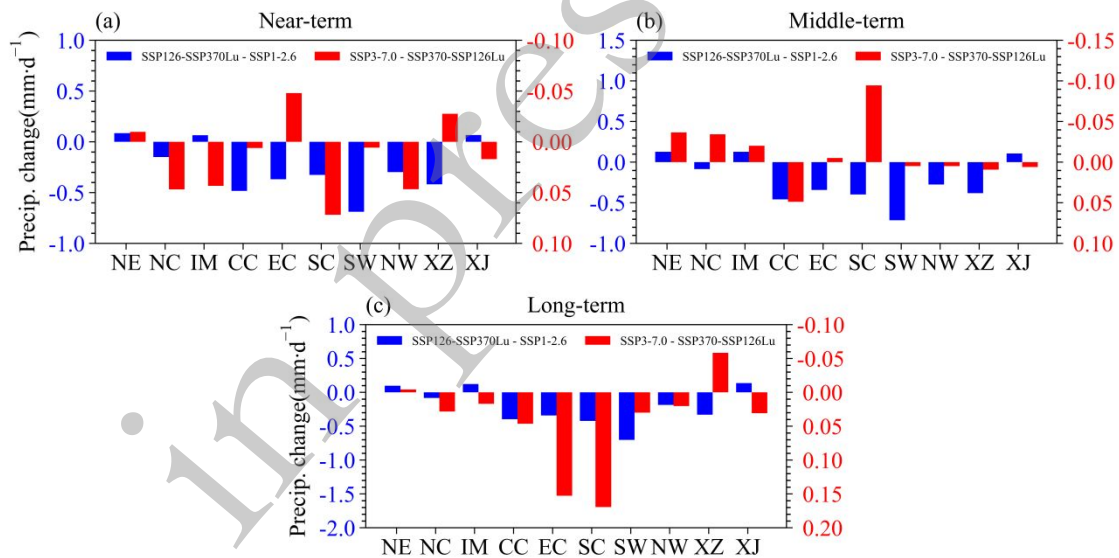
368 amplify the spatial difference on precipitation anomaly between the southern and
 369 northern China under the low radiative forcing scenario. However, under the
 370 medium/high radiative forcing scenario, the impacts of deforestation on precipitation
 371 changes in China are not significant, and the spatial differences are small.



372
 373 **Fig. 11.** Deforestation-induced annual mean precipitation changes ($\text{mm}\cdot\text{d}^{-1}$) in the near-
 374 term, middle-term, and long-term under (a-c) the low radiative forcing scenario, and
 375 (d-f) the medium/high radiative forcing scenario. The black dots indicate changes are
 376 statistically significant at a 0.05 confidence level.

377 Comparing the mean precipitation of 10 subregions in different periods, we find
 378 that, under the low radiative forcing scenario, deforestation-induced precipitation
 379 anomaly of all subregions has a relatively consistent pattern in the near-term, middle-
 380 term, and long-term (Fig. 12a-c). Except for the weak increase in northeast China, Inner
 381 Mongolia, and Xinjiang, deforestation reduces precipitation in other subregions.
 382 Regionally, the significant precipitation change is found in Xizang, southwest, central,

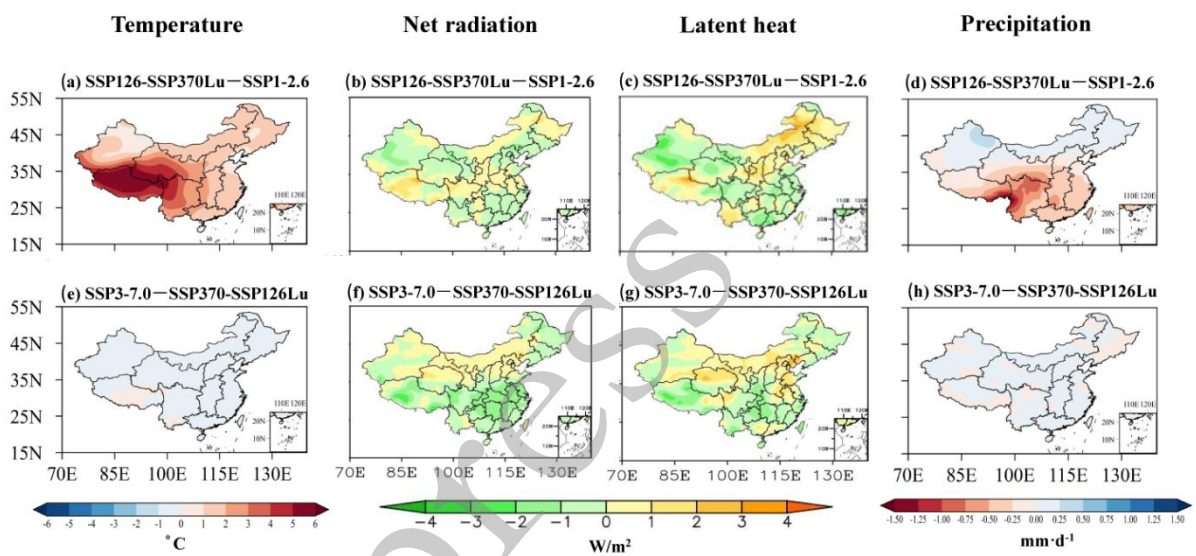
383 east and south China. However, under the medium/high radiative forcing scenario,
 384 deforestation-induced precipitation anomaly is less than $0.1 \text{ mm} \cdot \text{d}^{-1}$ in different periods
 385 over most subregions, and there are obvious regional differences. In the near-term, the
 386 mean precipitation would increase in south China, north China, Inner Mongolia and
 387 northwest China while decrease in northeast China, east China and Xizang (Fig. 12a).
 388 In the middle-term, precipitation decreases in south China with a magnitude of -0.1
 389 $\text{mm} \cdot \text{d}^{-1}$, and increases in southwest China with a magnitude of $0.08 \text{ mm} \cdot \text{d}^{-1}$ (Fig. 12b).
 390 In the long-term, except for the slight decrease in northeast China and Xizang, mean
 391 precipitation will increase in most subregions, especially in south and east China with
 392 a magnitude of $0.15 \text{ mm} \cdot \text{d}^{-1}$ (Fig. 12c).



393
 394 **Fig. 12.** Deforestation-induced annual mean precipitation changes ($\text{mm} \cdot \text{d}^{-1}$) in the (a)
 395 near-term, (b) middle-term, and (c) long-term over ten subregions under different
 396 emissions scenarios (blue bar: the low radiative forcing scenario, with values in the left
 397 y axis; red bar: the medium/high radiative forcing scenario, with values in the right
 398 axis).

399 **3.3 Mechanisms analysis**

400 Our results show that the impacts of deforestation on temperature and precipitation
 401 have different responses under different background climates. From the viewpoint of
 402 land surface energy budget and partitioning, we analyzed the changes of net radiation
 403 and latent/sensible heat fluxes associated with the variations of surface air temperature
 404 and precipitation under the different global warming scenarios.



405

406 **Fig. 13.** Deforestation-induced changes of annual mean (a, e) SAT ($^{\circ}\text{C}$), (b, f) net
 407 radiation (W/m^2), (c, g) latent heat (W/m^2), and (d, h) precipitation ($\text{mm}\cdot\text{d}^{-1}$) during
 408 2015-2099 over China under (a-d) the low radiative forcing scenario, and (e-h) the
 409 medium/high radiative forcing scenario.

410 As seen from Figure 13a-d, deforestation leads to a reduction in precipitation and
 411 latent heat fluxes in southern China under the low radiative forcing scenario. It is known
 412 that deforestation would lead to an increased albedo and hence a reduction in net
 413 radiation. In contrast, the drought caused by deforestation would lead to sensible heat
 414 fluxes increase, then warming the atmosphere. Therefore, deforestation has a greater

415 warming effect in the region with a larger decreased precipitation, here the impacts of
416 deforestation are dominantly controlled by hydrological processes rather than by albedo
417 changes. In northern China, deforestation would increase the precipitation under the
418 low radiative forcing scenario, and induce more latent heat release and a cooling effect.
419 In addition, warmer climates decrease snow and surface albedo, which increase the net
420 radiation and raise the temperature, thus partially negating the cooling due to
421 precipitation.

422 In contrast, as shown in Figure 13e-h, deforestation would increase the albedo and
423 decrease the net radiation in southern China under a warmer scenario. In contrast, the
424 increased precipitation would lead to latent heat fluxes increase in northwest China and
425 Inner Mongolia, and then affect the partitioned of net radiation between latent heat and
426 sensible heat fluxes, which eventually leads to a cooling effect in most parts of China.
427 It has an opposite response to the temperature changes under the low radiative forcing
428 scenario.

429 Pitman et al. (2011) proposed the background climate plays an important role in
430 determining the impacts of LULCC on regional climate. Hua and Chen (2013) and Li
431 et al. (2016) also investigated the mechanisms of regional impacts of LULCC on
432 climate changes with consideration of different atmospheric CO₂ concentrations. Their
433 results indicate that the level of CO₂ influences changes in surface albedo and
434 hydrometeorology, which determine the impacts of LULCC in the form of deforestation.
435 Our results are basically in line with the conclusions of previous studies, which
436 highlights the importance of interactions among the land surface energy balance,

437 terrestrial ecosystem, and hydrologic cycle for better understanding the overall impacts
438 of LULCC under changing climate background.

439 **4. Conclusions and discussion**

440 Based on the multi-model climate experiments from the Land Use Model
441 Intercomparison Project (LUMIP), this study investigates the climate responses of
442 temperature and precipitation in China to global forest area change under different
443 climate warming backgrounds.

444 The temperature changes due to deforestation have opposite responses under
445 different climate warming backgrounds. Under the low radiative forcing scenario,
446 deforestation would lead to an increase in the annual mean SAT and its interannual
447 variability and trend in all seasons. In contrast, deforestation would lead to cooling in
448 most parts of China, and decrease the interannual variability and trend of SAT under
449 the medium/high radiative forcing scenario, but the magnitude of temperature change
450 is less than that under the low radiative forcing scenario. Moreover, deforestation-
451 induced SAT change shows significant regional differences. Under the low radiative
452 forcing scenario, deforestation has a significant impact on SAT change in northwest
453 China, Xizang, and central China, while the significant subregions are central, south,
454 and east China under the medium/high radiative forcing scenario.

455 For precipitation, the responses to deforestation are also different under two
456 emissions scenarios. Under the low radiative forcing scenario, deforestation would lead
457 to significant increase in precipitation in northern China, but significant decrease in
458 southern China, especially during spring and summer. This precipitation pattern can be

459 found in the near-term (2021-2040), middle-term (2041-2070) and long-term (2071-
460 2099). However, under the medium/high radiative forcing scenario, changes in
461 precipitation are weaker, and there are no significant regional differences. Precipitation
462 increases are found over most parts of China both in the near-term and long-term, while
463 precipitation decreases are found in the middle-term, especially in south, north, and
464 northeast China.

465 In general, the impact of forest cover change on temperature and precipitation
466 under the low radiative forcing scenario is significantly greater than that under the
467 medium/high radiative forcing scenario. It is consistently shown that the background
468 climate plays an important role in the regional impact of forest cover change. Our
469 results show that under the low radiative forcing scenario, deforestation leads to
470 increased temperature and decreased precipitation in most parts of China, and the
471 effects are equivalent to the greenhouse effect. Therefore, under the low radiative
472 forcing scenario, afforestation would mitigate the effects of greenhouse gases to a
473 certain extent. However, under the higher emissions scenario, the response of
474 temperature and precipitation change over China is uncertain, and the magnitude is
475 negligible compared with the greenhouse gases effect indicating the afforestation could
476 not effectively improve the greenhouse gases effect in this scenario. This study reveals
477 the importance of different climate backgrounds in controlling LULCC effects on the
478 regional climate, and both changes need to be considered in future climate projection.
479 It should be noted that the analysis conducted in this study includes some preliminary
480 findings, and there are still some limitations and uncertainties worthy of further

481 investigation. The capacity of climate models to correctly capture the changes in rainfall
482 and temperature relative to LULCC probably affects many aspects of our results, which
483 presents a challenge for the development and improvement of climate models. In
484 addition, how the time evolution of LULCC affects local changes in rainfall and
485 temperature at regional scales is a problem deserving further study.

486 **Acknowledgments.** This study is jointly supported by the National Natural Science
487 Foundation of China under grant 41975081, the Research Funds for the Frontiers
488 Science Center for Critical Earth Material Cycling Nanjing University, and the
489 Fundamental Research Funds for the Central Universities (020914380103).

490 **Data Availability Statement.** The CMIP6 model data used in this study can be
491 accessed at the ESGF portal (<https://esgf-node.llnl.gov/projects/esgf-llnl/>).

492 REFERENCES

493 Alkama, R., and A. Cescatti, 2016: Biophysical climate impacts of recent changes in
494 global forest cover. *Science*, **351**, 600–604,
495 <https://doi.org/10.1126/science.aac8083>.

496 Arora, V. K., A. Montenegro, 2011: Small temperature benefits provided by realistic
497 afforestation efforts. *Nat. Geosci.*, **4**(8), 514-518,
498 <https://doi.org/10.1038/ngeo1182>.

499 Bonan, G. B., 2008: Forests and climate change: forcings, feedbacks, and the climate
500 benefits of forests. *Science*, **320**(5882), 1444-1449,
501 <https://doi.org/10.1126/science.1155121>.

502 Boysen, L. R., and Coauthors, 2020: Global climate response to idealized deforestation

503 in CMIP6 models. *Biogeosciences*, **17**(22), 5615-5638,
504 <https://doi.org/10.5194/bg-17-5615-2020>.

505 Bryan, B. A., and Coauthors, 2018: China's response to a national land-system
506 sustainability emergency. *Nature*, **559**, 193–204, [https://doi.org/10.1038/s41586-](https://doi.org/10.1038/s41586-018-0280-2)
507 [018-0280-2](https://doi.org/10.1038/s41586-018-0280-2).

508 Brovkin, V., and Coauthors, 2013: Effect of anthropogenic land-use and land-cover
509 changes on climate and land carbon storage in CMIP5 projections for the twenty-
510 first century. *J. Climate*, **26**(18), 6859-6881, [https://doi.org/10.1175/jcli-d-12-](https://doi.org/10.1175/jcli-d-12-00623.1)
511 [00623.1](https://doi.org/10.1175/jcli-d-12-00623.1).

512 Chen, H. S., X. Li, and W. J. Hua, 2015: Numerical simulation of the impact of land
513 use/land cover change over China on regional climates during the last 20 year.
514 *Chinese Journal of Atmospheric Sciences*, **39**(2), 357-369,
515 <https://doi.org/10.3878/j.issn.1006-9895.1404>. (in Chinese)

516 Davin, E. L., and N. de Noblet-Ducoudré, 2010: Climatic impact of global-scale
517 deforestation: Radiative versus nonradiative processes. *J. Climate*, **23**, 97-112,
518 <https://doi.org/10.1175/2009JCLI3102.1>.

519 Devaraju, N., N. de Noblet-Ducoudré, B. Quesada, and G. Bala, 2018: Quantifying the
520 relative importance of direct and indirect biophysical effects of deforestation on
521 surface temperature and teleconnections. *J. Climate*, **31**, 3811–3829,
522 <https://doi.org/10.1175/JCLI-D-17-0563.1>.

523 Dixon, R. K., and Coauthors, 1994: Carbon pools and flux of global forest ecosystems.
524 *Science*, **263**, 185-190.

525 FAO, 2009: *State of the World's Forests 2009*. Rome, Italy, 168pp.
526 www.fao.org/docrep/011/i0350e/i0350e00.htm.

527 Foley, J. A., and Coauthors, 2005: Global consequences of land use. *Science*, **309**(5734),
528 570-574, <https://doi.org/10.1126/science.1111772>.

529 Fu, B., S. Wang, Y. Liu, J. Liu, W. Liang, and C. Miao, 2017: Hydrogeomorphic
530 ecosystem responses to natural and anthropogenic changes in the Loess Plateau of
531 China. *Annu. Rev. Earth Planet. Sci.*, **45**, 223–243,
532 <https://doi.org/10.1146/annurev-earth-063016-020552>.

533 Ge, J., and Coauthors, 2019: The nonradiative effect dominates local surface
534 temperature change caused by afforestation in China. *J. Climate*, **32**, 4445-4471,
535 <https://doi.org/10.1175/JCLI-D-18-0772.1>.

536 Held, I. M., and B. J. Soden, 2006: Robust responses of the hydrological cycle to global
537 warming. *J. Climate*, **19**, 5686-5690, <https://doi.org/10.1175/JCLI3990.1>.

538 Hong, T., J. J. Wu, X. B. Kang, M. Yuan, and L. Duan, 2022: Impacts of Different Land
539 Use Scenarios on Future Global and Regional Climate Extremes. *Atmosphere*, **13**,
540 <https://doi.org/10.3390/atmos13060995>.

541 Hu, Z. H., Z. F. Xu, and Z. G. Ma, 2018: The impact of land use/land cover changes
542 under different greenhouse gas concentrations on climate in Europe. *Climatic and
543 Environmental Research*, **23**(2), 176-184, <https://doi.org/10.3878/j.issn.1006-9585.2017.17010>. (in Chinese)
544

545 Hua, W. J., and H. S. Chen, 2013: Recognition of climatic effects of land use/land cover
546 change under global warming. *Chinese Science Bulletin*, **58**(31), 3852–3858,
547 <https://doi.org/10.1007/s11434-013-5902-3>.

548 Hua, W. J., H. S. Chen, and X. Li, 2015: Effects of future land use change on the
549 regional climate in China. *Science China: Earth Sciences*, **45**, 1034-1042,
550 <https://doi.org/10.1007/s11430-015-5082-x>. (in Chinese)

551 Hua, W. J., and Coauthors, 2017: Observational quantification of climatic and human
552 influences on vegetation greening in China. *Remote Sens.*, **9**(5), 425,
553 <https://doi.org/10.3390/rs9050425>.

554 Hua, W. J., S. Y. Liu, and H. S. Chen, 2021: Short commentary on Land Use Model
555 Intercomparison Project (LUMIP). *Trans. Atmos. Sci.*, **44**(6), 818-824,
556 <https://doi.org/10.13878/j.cnki.dqkxxb.20210413001>. (in Chinese)

557 Huang, H., Y. Xue, N. Chilukoti, Y. Liu, G. Chen, and I. Diallo, 2020: Assessing global
558 and regional effects of reconstructed land-use and land-cover change on climate
559 since 1950 using a coupled land-atmosphere-ocean model. *J. Climate*, **33**(20),
560 8997-9013, <https://doi.org/10.1175/jcli-d-20-0108.1>.

561 Hurtt, G. C., and Coauthors, 2006: The underpinnings of land-use history: Three
562 centuries of global gridded land-use transitions, wood-harvest activity, and
563 resulting secondary lands. *Global Change Biology*, **12**(7), 1208-1229,
564 <https://doi.org/10.1111/j.1365-2486.2006.01150.x>.

565 IPCC, 2021: *Climate Change 2021: The Physical Science Basis [M]// Contribution of*
566 *Working Group I to the Sixth Assessment Report of the IPCC*. Masson-Delmotte,

567 V. et al., Eds. Cambridge University Press, 3949pp.

568 Lawrence, P. J., and Coauthors, 2012: Simulating the biogeochemical and
569 biogeophysical impacts of transient land cover change and wood harvest in the
570 Community Climate System Model (CCSM4) from 1850-2100. *J. Climate*, **25**(9),
571 3071-3095, <https://doi.org/10.1175/jcli-d-11-00256.1>.

572 Lawrence, D. M., and Coauthors, 2016: The land use model intercomparison project
573 (LUMIP) contribution to CMIP6: rationale and experimental design. *Geosci.*
574 *Model. Dev.*, **9**(9), 2973-2998, <https://doi.org/10.5194/gmd-9-2973-2016>.

575 Lee, X., and Coauthors, 2011: Observed increase in local cooling effect of deforestation
576 at higher latitudes. *Nature*, **479**(7373), 384-387,
577 <https://doi.org/10.1038/nature10588>.

578 Li, Y., and Coauthors, 2015: Local cooling and warming effects of forests based on
579 satellite observations. *Nat. Commun.*, **6**, 6603,
580 <https://doi.org/10.1038/ncomms7603>.

581 Li, Y., and Coauthors, 2016: The role of spatial scale and background climate in the
582 latitudinal temperature response to deforestation. *Earth System. Dynamics*, **7**(1),
583 167-181, <https://doi.org/10.5194/esd-7-167-2016>.

584 Liu, J., S. Li, Z. Ouyang, C. Tam, and X. Chen, 2008: Ecological and socioeconomic
585 effects of China's policies for ecosystem services. *Proc. Natl. Acad. Sci. USA*, **105**,
586 9477-9482, <https://doi.org/10.1073/pnas.0706436105>.

587 Lorenz, R., A. Pitman, and S. A. Sisson, 2016: Does Amazonian deforestation cause
588 global effects; can we be sure? *J. Geophys. Res: Atmos.*, **121**(10), 5567-5584,

589 <https://doi.org/10.1002/2015jd024357>.

590 Luo, X., and Coauthors, 2022: The biophysical impacts of deforestation on
591 precipitation: results from the CMIP6 model intercomparison. *J. Climate*, **35**,
592 3293-3311, <https://doi.org/10.1175/JCLI-D-21-0689.1>.

593 Mao, H. Q., X. D. Yan, and Z. Xiong, 2011: An overview of impacts of land use change
594 on climate. *Climatic and Environmental Research*, **16**(4), 513–524,
595 <https://doi.org/10.3878/j.issn.1006-9585.2011.04.12>.

596 Perugini, L., L. Caporaso, S. Marconi, A. Cescatti, B. Quesada, N. de Noblet-Ducoudré,
597 J. I. House, and A. Arneth, 2017: Biophysical effects on temperature and
598 precipitation due to land cover change. *Environ. Res. Lett.*, **12**, 053002,
599 <https://doi.org/10.1088/1748-9326/aa6b3f>.

600 Pielke, R. A., and R. Avissar, 1990: Influence of landscape structure on local and
601 regional climate. *Landscape Ecology*, **4**(2), 133-155.

602 Pielke, R. A., and Coauthors, 2011: Land use/land cover changes and climate: modeling
603 analysis and observational evidence. *Clim. Change*, **2**(6), 828-850,
604 <https://doi.org/10.1002/wcc.144>.

605 Pitman, A. J., and Coauthors, 2009: Uncertainties in climate responses to past land
606 cover change: First results from the LUCID intercomparison study. *Geophys. Res.*
607 *Lett.*, **36**, L1481, <https://doi.org/10.1029/2009GL039076>.

608 Pitman, A. J., F. B. Avila, G. Abramowitz, Y. P. Wang, S. J. Phipps, and N. de Noblet-
609 Ducoudré, 2011: Importance of background climate in determining impact of

610 land-cover change on regional climate. *Nature Climate Change*, **1**, 472–475,
611 <https://doi.org/10.1038/nclimate1294>.

612 Pitman, A. J., and Coauthors, 2012: Effects of land cover change on temperature and
613 rainfall extremes in multi-model ensemble simulations. *Earth System Dynamics*,
614 **3**, 213–231, <https://doi.org/10.5194/esd-3-213-2012>.

615 Schuenemann, K. C., and J. J. Cassano, 2009: Changes in synoptic weather patterns
616 and Greenland precipitation in the 20th and 21st centuries: 1. Evaluation of late
617 20th century simulations from IPCC models. *J. Geophys. Res.*, **114**: D20113,
618 <https://doi.org/10.1029/JD011705>.

619 Shao, P., and X. D. Zeng, 2012: Progress in the study of the effects of land use and land
620 cover change on the climate system. *Climatic and Environmental Research*,
621 **17**(1), 103-111, <https://doi.org/10.3878/j.issn.1006-958>. (in Chinese)

622 Sun, G. D., and M. Mu, 2013: Using the Lund-Potsdam-Jena model to understand the
623 different responses of three woody plants to land use in China. *Adv. Atmos. Sci.*,
624 **30**(2), 515-524, <https://doi.org/10.1007/s00376-012-2011-1>.

625 Taylor, C. M., and Coauthors, 2002: The Influence of Land Use Change on Climate in
626 the Sahel. *J. Climate*, **15**(24), 3615-3629.

627 Tian, L., Z. H. Jiang, and W. L. Chen, 2016: Evaluation of summer average circulation
628 simulation over East Asia by CMIP5 climate models. *Climatic and Environmental*
629 *Research*, **21**(4), 380-392, <https://doi.org/10.3878/j.issn.1006-9585.2016.13089>.
630 (in Chinese)

631 Wan, H. C., and Z. Zhong, 2014: Ensemble simulations to investigate the impact of

632 large-scale urbanization on precipitation in the lower reaches of Yangtze River
633 Valley, China. *Quart. J. Royal. Meteor. Soc.*, **140**, 258-266,
634 <https://doi.org/10.1002/qj.2125>.

635 Wang, A. H., Y. Miao, and X. L. Shi, 2021: Short commentary on the Land-Use Model
636 Intercomparison Project (LUMIP). *Climate Change Research*, **17**(3), 367-373,
637 <https://doi.org/10.12006/j.issn.1673-1719.2020.170>. (in Chinese)

638 Xu, Z. F., and Coauthors, 2015: Investigating diurnal and seasonal climatic response to
639 land use and land cover change over monsoon Asia with the community earth
640 system model, *J. Geophys. Res: Atmos.*, **120**, 1137-1152,
641 <https://doi.org/10.1002/2014JD022479>.

642 Xu, Z. F., and Z. L. Yang, 2017: Relative impacts of increased greenhouse gas
643 concentrations and land cover change on the surface climate in arid and semi-arid
644 regions of China. *Climatic Change*, **144**: 491-503, [https://doi.org/10.1007/s10584-](https://doi.org/10.1007/s10584-017-2025-x)
645 [017-2025-x](https://doi.org/10.1007/s10584-017-2025-x).

646 Yang, X. C., Y. L. Zhang, and L. S. Liu, 2009: Sensitivity of surface air temperature
647 change to land types in China. *Sci. China Ser. D-Earth Sci.*, **39**(5), 638-646,
648 <https://doi.org/10.1007/s11430-009-0085-0>. (in Chinese)

649 Yang, X. C., and Coauthors, 2010: Observational evidence of the impact of vegetation
650 cover on surface air temperature change in China. *Chinese J. Geophys.*, **53**(4),
651 838-841, <https://doi.org/10.3969/j.issn.0001-5733.2010.04.008>. (in Chinese)

652 Yuan, Y. F., P. M. Zhai, 2022: Latest understanding of extreme weather and climate
653 events under global warming and urbanization influences. *Trans. Atmos. Sci.*,

654 45(2), 161-166, <https://doi.org/10.13878/j.cnki.dqkxxb.20211011001>. (in
655 Chinese)
656 Zhu, H. H., Y. Zhang, X. Y. Shen, S. Y. Wang, L. Y. Shang, Y. Q. Su, 2018: A
657 numerical simulation of the impact of vegetation evolution on the regional climate
658 in the ecotone of agriculture and animal husbandry over China. *Plateau
659 Meteorology*, 37(3), 721-733, [https://doi.org/10.7522/j.issn.1000-
0534.2018.00050](https://doi.org/10.7522/j.issn.1000-
660 0534.2018.00050). (in Chinese)

in press